



# Use of UV–vis–NIR spectroscopy to monitor label-free interaction between molecular recognition elements and erythropoietin on a gold-coated polycarbonate platform



Marimuthu Citartan<sup>a</sup>, Subash C.B. Gopinath<sup>a,b,c,\*</sup>, Junji Tominaga<sup>b</sup>, Yeng Chen<sup>c</sup>,  
Thean-Hock Tang<sup>a,\*\*</sup>

<sup>a</sup> Advanced Medical & Dental Institute (AMDI), Universiti Sains Malaysia, 13200 Kepala Batas, Penang, Malaysia

<sup>b</sup> Nanoelectronics Research Institute, National Institute of Advanced Industrial Science & Technology, 1-1-1 Higashi, Tsukuba, Ibaraki 305-8562, Japan

<sup>c</sup> OCRCC, Faculty of Dentistry, University of Malaya, 50603 Kuala Lumpur, Malaysia

## ARTICLE INFO

### Article history:

Received 29 January 2014

Received in revised form

16 March 2014

Accepted 17 March 2014

Available online 24 March 2014

### Keywords:

Erythropoietin  
Spectroscopy  
Polycarbonate  
Antibody  
Aptamer

## ABSTRACT

Label-free-based detection is pivotal for real-time monitoring of biomolecular interactions and to eliminate the need for labeling with tags that can occupy important binding sites of biomolecules. One simplest form of label-free-based detection is ultraviolet–visible–near-infrared (UV–vis–NIR) spectroscopy, which measure changes in reflectivity as a means to monitor immobilization and interaction of biomolecules with their corresponding partners. In biosensor development, the platform used for the biomolecular interaction should be suitable for different molecular recognition elements. In this study, gold (Au)-coated polycarbonate was used as a platform and as a proof-of-concept, erythropoietin (EPO), a doping substance widely abused by the athletes was used as the target. The interaction of EPO with its corresponding molecular recognition elements (anti-EPO monoclonal antibody and anti-EPO DNA aptamer) is monitored by UV–vis–NIR spectroscopy. Prior to this, to show that UV–vis–NIR spectroscopy is a suitable method for measuring biomolecular interaction, the interaction between biotin and streptavidin was demonstrated via this strategy and reflectivity of this interaction decreased by 25%. Subsequent to this, interaction of the EPO with anti-EPO monoclonal antibody and anti-EPO DNA aptamer resulted in the decrease of reflectivity by 5% and 10%, respectively. The results indicated that Au-coated polycarbonate could be an ideal biosensor platform for monitoring biomolecular interactions using UV–vis–NIR spectroscopy. A smaller version of the Au-coated polycarbonate substrates can be derived from the recent set-up, to be applied towards detecting EPO abuse among athletes.

© 2014 Elsevier B.V. All rights reserved.

## 1. Introduction

Label-free-based monitoring of biomolecular interactions is a popular alternative to label-associated procedures (e.g., fluorescence, luminescence, and radioactivity). Label-free methods avoid the need for labeling with tags that can occupy important binding sites of the biomolecules. One promising label-free methodology is ultraviolet–visible–near-infrared (UV–vis–NIR) spectroscopy, which measures the reflectivity and scattering of light from the substrate surface as a function of wavelength. Each material has a distinct reflectivity spectrum due to the thickness, refractive index, and absorption

coefficient of the substrate. Thus, adsorption of molecular recognition elements (MREs) on the substrate surface (for example gold) and the subsequent interaction of the MRE with the target alter the reflectivity, which can be tracked in real time. MREs are biomolecules (e.g., DNA, RNA, or protein) that can bind a target with high affinity and specificity. Antibodies are widely used due to their molecular recognition properties and because they can be generated against any target molecule that can elicit immunogenicity. Another group of MREs, termed aptamers, is specific nucleic acid sequences that can bind a wide variety of targets with high affinity and specificity [1]. This class of molecules is generated by a Systematic Evolution of Ligands by Exponential Enrichment (SELEX) system and can be raised against any target molecule (including non-immunogenic molecules) [2–5]. Implementation of these MREs in biosensor development requires suitable platforms for molecular immobilization.

The platform chosen must be able to correctly orientate biomolecules for immobilization onto its surface. As the most electronegative metal, gold (Au) meets this criteria. Au is easily

\* Corresponding author at: Advanced Medical & Dental Institute (AMDI), Universiti Sains Malaysia, 13200 Kepala Batas, Penang, Malaysia.  
Tel.: +604 5622302; fax: +604 5622349.

\*\* Corresponding author Tel.: +604 5622302; fax: +604 5622349.

E-mail addresses: [gopis11@gmail.com](mailto:gopis11@gmail.com) (S.C.B. Gopinath),  
[tangth@amdi.usm.edu.my](mailto:tangth@amdi.usm.edu.my) (T.-H. Tang).

prepared and can be patterned using a combination of lithographic tools and chemical etchants. In addition, the optical, electronic, and magnetic properties of Au are in sync with the optimum biomolecular interactions (DNA/RNA/protein), which makes Au the preferred platform in the field of nanoscience and nanotechnology. However, in order to use an Au layer as the platform for immobilization of both antibodies and aptamers, solid support for the layer is needed. Because Au can be easily removed when treated with buffering solution [6], the solid support must be very resistant to chemical reaction. Moreover, it needs to be light and inexpensive to produce. Polycarbonate appears to be a suitable material to provide solid support to Au for immobilization of biomolecules.

In this study, we developed an Au-coated polycarbonate sensor platform and used UV-vis-NIR spectroscopy to measure the interaction between MREs (an anti-erythropoietin (EPO) antibody and an anti-EPO DNA aptamer), which were immobilized on the surface of the platform, with the target EPO. These MREs are useful for capturing and detecting the presence of EPO. As a glycoprotein hormone produced by the kidney, EPO is the erythropoietic growth factor responsible for erythroid differentiation, survival, and proliferation [7]. With the advent of recombinant DNA technology, the gene that encodes EPO (located on chromosome 7) was cloned and expressed in a Chinese hamster ovary cell line to produce recombinant human EPO (rHuEPO). This substance, which is used for the treatment of patients with renal failure, has been illegally used in endurance sports to improve the oxygen carrying capacity of blood [8]. The use of performance enhancing drugs, known as doping, gives athletes an unfair advantage over their competitors. Thus, drug testing of athletes is needed to ensure an even playing field. Developing a sensing system equipped with a simple form of detection would aid in detection of EPO abuse by athletes and would likely prove useful for many other types of analysis. Our proposed biosensor based on MREs against EPO should facilitate specific detection and capture of EPO.

## 2. Materials and methods

### 2.1. Materials

Anti-EPO monoclonal antibody and recombinant human EPO alpha (rHuEPO- $\alpha$ ) were obtained from ProSpec-Tany TechnoGene Ltd. (Ness-Ziona, Israel). AuNPs (40 nm diameter) were purchased from BBInternational (Cardiff, UK), and 40 nm AuNP-streptavidin conjugates (15 O.D.) were acquired from BioAssay Works (Maryland, USA). Ethanamine, 3,3',5,5'-tetramethylbenzidine (TMB) substrate, N-hydroxysuccinimide (NHS), 16-mercaptohexadecanoic acid (MHA), and 1-ethyl-3-[3-dimethylaminopropyl] carbodiimide hydrochloride (EDC) were purchased from Sigma Aldrich (St. Louis, USA). Anti-EPO DNA aptamers (previously generated against rHuEPO- $\alpha$ ) tagged with poly dA<sub>24</sub> [5], biotin conjugated to thiolated poly dT<sub>10</sub> (biotin-dT<sub>10</sub>-thiol) and thiolated poly dT<sub>20</sub> were commercially synthesized (Tsukuba Oligo Service (Tsukuba, Japan)). Polyvinylidene fluoride (PVDF) membranes (85 × 90 mm<sup>2</sup>) and 5%–20% gradient polyacrylamide gel (SuperSep™ 5%–20% gel) were purchased from Atta (Tokyo, Japan) and Wako Chemicals (Osaka, Japan), respectively. Microcon centrifugal filter devices with 10 kDa cut-off membrane were obtained from Millipore (Billerica, USA).

### 2.2. Sputtering

Sputtering of Au material onto the surface of the polycarbonate was carried out in a clean room using an RF-magnetron reactive sputtering machine (CFS-4EP-LL, Shibaura, Japan). Before sputtering, the polycarbonate surface was cleaned with nitrogen (N<sub>2</sub>) gas

using an air gun. The sputtering power was 50 W, and the sputtering was carried out in an argon (Ar) gas atmosphere of 0.5 Pa. The gas flow rate of Ar was regulated at 10 sccm. Different thicknesses of Au layers (5, 10, 30, and 50 nm) were sputtered onto the surface of polycarbonate by varying the duration of sputtering. Following sputtering, materials were kept under dry and dust-free conditions.

### 2.3. Gel shift assay

A gel shift assay was performed to examine the interaction of the anti-EPO DNA aptamer with the target protein. First, 4  $\mu$ M of anti-EPO DNA aptamer (dissolved in 1x HEPES buffer) was heated at 95 °C for 2 min, followed by cooling to room temperature (RT) for 10 min. This was followed by the addition of MgCl<sub>2</sub> to a final concentration of 5 mM and EPO at concentrations ranging from 0 to 16  $\mu$ M for each of 4  $\mu$ M of the DNA aptamer. Each of these binding reactions was carried out in 10  $\mu$ L reaction volume. Incubation was performed at RT for 15 min. Prior to electrophoresis on 12% native PAGE at 140 V for 1 h, 1  $\mu$ L of 90% glycerol was added into each reaction mixture. Before loading the reaction mixtures, the gel was subjected to pre-run at 160 V for 10 min. The gel was stained in 1 × TAE buffer (40 mM Tris acetate, 1 mM EDTA, pH 8.0) containing 0.5  $\mu$ g mL<sup>-1</sup> of ethidium bromide.

### 2.4. UV-vis-NIR spectroscopy

A UV-vis-NIR spectrophotometer (Shimadzu-MPC-3100, Kyoto, Japan) was used to examine the spectral changes associated with different thicknesses of Au (5, 10, 30, and 50 nm) sputtered onto the surface of the polycarbonate. Spectroscopy was also used to monitor the binding of anti-EPO antibody and anti-EPO DNA aptamer to the target EPO by measuring reflectivity changes over wavelengths from 300 to 1400 nm. The baseline was adjusted accordingly while the reflection mode was set and nullified with a basic signal. The data was graphed using Microsoft Excel spreadsheet. Reflectivity was determined based on the highest point of reflectivity obtained from the graph (reflectivity versus wavelength).

### 2.5. Western blot analysis

Western blot analysis was carried out to evaluate the specific interaction between EPO and the anti-EPO antibody. Different amounts of EPO (9.76 × 10<sup>-4</sup>, 1.95 × 10<sup>-3</sup>, 3.91 × 10<sup>-3</sup>, 7.81 × 10<sup>-3</sup>, 1.56 × 10<sup>-2</sup>, 3.12 × 10<sup>-2</sup>, 6.25 × 10<sup>-2</sup>, and 1.25 × 10<sup>-1</sup>  $\mu$ g) were run on the 5%–20% gradient polyacrylamide gel and subsequently transferred to the PVDF membrane by using a semi-dry transfer method with the aid of transfer buffer (25 mM Tris-base, 150 mM glycine, 10% methanol). The membrane was then incubated in blocking buffer (3% skim milk, 10 mM Tris-Cl, pH 7.5, 0.15 M NaCl) for 30 min, followed by washing three times with washing buffer (10 mM Tris-Cl, pH 7.5, 0.15 M NaCl, 0.05% Tween-20). Next, the membrane was incubated with 0.1  $\mu$ g/mL of anti-EPO antibody for 16 h, washed again three times with washing buffer, and incubated for 30 min with secondary antibody (goat-anti-mouse conjugated horseradish peroxidase at the dilution of 1:2500). Detection was performed in 5 mL of TMB substrate for 5 min.

### 2.6. Amino-thiol coupling reaction and pH scouting

Ten microliters of 5 mM MHA, 100  $\mu$ L of 130 mM NHS, and 100  $\mu$ L of 400 mM EDC were mixed and incubated at RT for 10 min. Anti-EPO antibody was added to a final concentration of 100 nM and incubated for 30 min at RT. These mixtures were then passed through Microcon centrifugal filter devices with the 10 kDa

cut-off membrane to remove the unbound MHA, NHS, and EDC by centrifugation for 1 h at  $3000 \times g$ . The antibodies retained on the membrane were recovered using sodium acetate buffer with different pH values (4.0, 4.5, 5.0, and 5.5). The recovered antibodies were spotted onto the surface of Au-coated polycarbonate, incubated for 30 min at RT, and washed three times with 200  $\mu\text{L}$  of 1x HEPES-KOH, pH 7.5 (10 mM HEPES, 150 mM NaCl, pH 7.5). The same procedure of amino-thiol coupling was performed for immobilization of EPO onto AuNPs.

### 2.7. Conjugation of EPO to AuNPs

In this study, MHA conjugated EPO was attached to AuNPs with a diameter of 40 nm. Initially, 10 mM phosphate buffered saline (PBS) (137 mM NaCl, 2.7 mM KCl, 10 mM  $\text{Na}_2\text{HPO}_4$ , 2 mM  $\text{KH}_2\text{PO}_4$ ) containing AuNPs was centrifuged to sediment AuNPs. After removing the buffer, 100  $\mu\text{L}$  of sodium acetate buffer containing 100 nM EPO (prepared by amino-thiol coupling reaction) was added and pipetted several times to resuspend AuNPs. The suspension was incubated for 1 h at RT on a shaking rotating platform. The suspension was then centrifuged, the buffer was removed, and AuNPs were resuspended in 100  $\mu\text{L}$  of 10 mM PBS buffer, pH 7.4.

### 2.8. Interaction of streptavidin-tagged AuNPs with thiolated biotin on Au-coated polycarbonate

To test the interaction of streptavidin-tagged AuNPs with thiolated biotin on Au-coated polycarbonate, 100 nM of biotin-dT<sub>10</sub>-thiol was added to the surface of 30 nm Au-coated polycarbonate and incubated for 30 min at RT. The sample was then washed three times with 200  $\mu\text{L}$  of 10 mM PBS buffer. Reflectivity was measured and AuNP-streptavidin conjugates equivalent to 1 O.D. were added for incubation at RT for 10 min. The sample was washed again and UV-vis-NIR spectrophotometer readings were taken.

### 2.9. Interaction of anti-EPO antibody, anti-EPO DNA aptamer, and EPO on the Au-coated polycarbonate platform

To analyze the interaction between anti-EPO antibody and EPO on the surface of Au-coated polycarbonate, the amino-thiol coupling interaction was performed as described above. The antibodies on the surface of the Amicon device's membrane were recovered in sodium acetate buffer of appropriate pH based on the results of the pH scouting experiment. The recovered antibodies were spotted onto the surface of Au-coated polycarbonate and incubated for 30 min at RT followed by washing. Following spectrophotometric reading, 100 nM of AuNP-tagged EPO was added, incubated for 30 min, and washed before the reflectivity measurement was taken.

The anti-EPO DNA aptamer tagged with poly dA<sub>24</sub> was dissolved to a final concentration of 1  $\mu\text{M}$  in 100  $\mu\text{L}$  of volume, heated at 95 °C for 2 min in the presence of an equal amount of thiol-dT<sub>20</sub> and cooled to RT for 10 min. The mixture was pipetted onto the surface of Au-coated polycarbonate and incubated at RT for 30 min. After washing three times with 10 mM PBS, EPO was added to a final concentration of 290 nM and incubated at RT for 30 min. After washing with 10 mM PBS, the reflectivity measurement was taken.

### 2.10. Nanoscale imaging

Nanoscale imaging of the interaction of AuNP tagged EPO and the anti-EPO antibody immobilized on the surface of Au-coated polycarbonate was executed using an (L-trace) SPA-500k Atomic

Force Microscope (AFM) (Seiko Instruments Inc., Chiba, Japan) and a JSM-6240F Field Emission Scanning Electron Microscope (FE SEM), (JEOL Ltd., Tokyo, Japan). AFM images were acquired using tapping modes via a classic silicon or silicon nitride cantilever. Imaging was carried out in air at RT with relative humidity lower than 5%. Equivalently, nanoscale imaging was also performed on the interaction of streptavidin-tagged AuNPs and thiolated biotin on the surface of Au-coated polycarbonate.

## 3. Results and discussion

### 3.1. Evaluating Au layer thickness by reflection analysis

UV-vis-NIR spectroscopy measurements can provide information about the reflection properties of any material as a function of wavelength. These measurements can help determine the suitability of substrates for use as sensors based on their optical properties. Polycarbonate, which consists of long chain linear polyesters of carbonic acid and dihydric phenols, is a good substrate due to the presence of a phenyl group and two methyl side groups on the molecular chain. These properties result in good thermal resistance and prevent the polycarbonate from developing a crystalline structure, thus permitting transparency [9]. Polycarbonate with a thickness of 0.6 mm was chosen as the surface on which the layer of Au material sputtered. In the presence of a reflection mirror, the reflectivity of this surface was 90% (reflectance), whereas without the mirror the reflectivity was 10% (transmittance) (Fig. 1A). Thus polycarbonate of this thickness (0.6 mm) allows almost 100% reflectivity with low scattering or absorption losses [10].

Au sputtering, which is the process by which a very thin layer of Au is created by gradual deposition of Au on the platform surface, was carried out next. Au layers with four different thicknesses (5, 10, 30, and 50 nm) were created, and then reflectance measurements were taken both in the presence and absence of the reflection mirror. Maximum reflections of 35%, 60%, 90%, and 100% were recorded for Au thicknesses of 5, 10, 30, and 50 nm, respectively (with the reflection mirror) (Fig. 1B). Without the reflection mirror, reflectivity values of ~25%, 40%, 68%, and 70% were measured for that of 5, 10, 30, and 50 nm thick Au layers, respectively (Fig. 1C). Based on these data, 30 and 50 nm thick Au layers were considered to be the most suitable for use in the biosensor. These thicknesses ensure that the reflectivity measurements used to monitor biomolecular interactions on the surface of the Au layer to be accurate without the use of a mirror. Ultimately, 30 nm thick Au layer is preferable because it costs less to produce, thereby minimizing the overall cost of the sensing plate (Inset Fig. 1).

### 3.2. Amino-thiol coupling and pH scouting

Adsorption of protein molecules onto any surface via intermolecular forces (mainly by ionic bonds, hydrophobic and polar interactions) will result in heterogeneous and randomly oriented immobilized protein molecules. These protein molecules create many contacts in different orientations that lessen the repulsive interaction with the surface and other molecules. Therefore, well-defined immobilization through functionalization of protein molecules coupled with tailoring of the immobilized surface is a requisite for reproducible and oriented immobilization [11]. Hence, to attach anti-EPO antibody to the surface of Au-coated polycarbonate in a well-ordered orientation, the amino coupling reaction that links the antibody to MHA was performed [12]. MHA, which is a carboxylic acid containing a carboxyl group and thiol

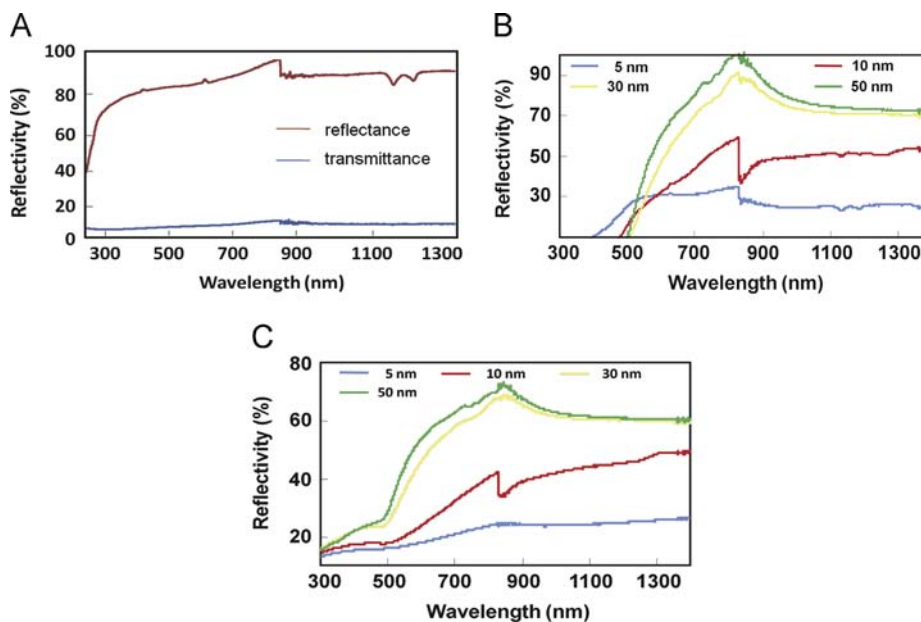


**Fig. 1.** (A) UV–vis–NIR measurement of polycarbonate of 0.6 mm thickness. (B) Reflectance measurements for 5, 10, 30, and 50 nm thick Au layers in the presence of a reflection mirror. (C) Reflectance measurements for 5, 10, 30, and 50 nm thick Au layers in the absence of a reflection mirror.

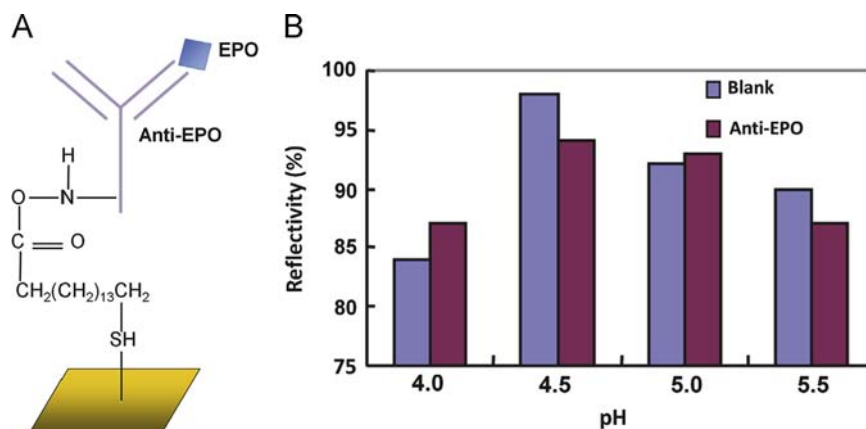


**Fig. 2.** (A) Immobilization of anti-EPO antibody on the surface of Au-coated polycarbonate followed by capturing of EPO. (B) Analysis of pH scouting of immobilization of anti-EPO antibody on the surface of Au-coated polycarbonate.

group at both ends, forms self-assembled monolayers on the Au surface [13]. Hence, conjugation of the anti-EPO antibody's amino group to the carboxyl group of the MHA allows immobilization of the antibody onto the Au surface via the thiol group at the other extremity of the MHA. The thiol group, which contains a sulfur (S) atom, has strong affinity for Au atom, thus forming an Au–S bond [14]. In this study, we used EDC (a carbodiimide zero cross-linker) to facilitate the direct conjugation of the carboxylic group of MHA to the amines of the anti-EPO antibody. NHS increases the efficiency of the EDC-mediated coupling reaction up to 20-fold, as the addition of this substrate converts the carboxyl group to the reactive succinimide ester, which then forms a stable amide bond with the amine group of the anti-EPO antibody [15]. In short, utilization of MHA enabled the immobilization of both anti-EPO antibody and EPO antigen on the surface of Au-coated flat surfaces and AuNPs, respectively, by adopting the stand-up configuration to effectively capture target molecules (Fig. 2A) [16].

pH scouting was also conducted to determine which pH of sodium acetate buffer (4.0, 4.5, 5.0, and 5.5) was best for the immobilization of thiolated protein on Au surface. At pH 4.5, anti-EPO

linked-MHA had the best conjugation capacity on the surface of Au-coated polycarbonate (Fig. 2B). Upon attachment of anti-EPO antibody to the surface of Au-coated polycarbonate, the reflectivity decreased by about 6% (from 99% to 93%) for pH 4.5, but the reflectivity change was still higher compared to that of pH 5.5, where the reflectivity dropped by only 3% (90% to 87%). For pH 4.0 and 5.0, the reflectivity increased when anti-EPO antibody was spotted onto the surface of Au-coated polycarbonate, implying that the immobilization of anti-EPO antibody with these two pHs was unsuccessful. Reactivity and selectivity of the thiol groups are influenced by pH and pKa of the anti-EPO antibody, creating electrostatic environment that modulates pKa of thiol groups [17]. Subsequent to immobilization of anti-EPO antibody, washing was performed to remove any unbound antibody that might have been absorbed non-specifically on the surface of the Au layer. Such non-specific absorption of the antibody can occur via a variety of protein–surface mechanisms (i.e., electrostatic interaction, hydrogen bonding, hydrophobic interaction, and a combination of these) [18]. Sodium acetate buffer of pH 4.5 was chosen for the immobilization of the thiolated anti-EPO antibody onto the surface of Au-coated polycarbonate (Inset Fig. 2).

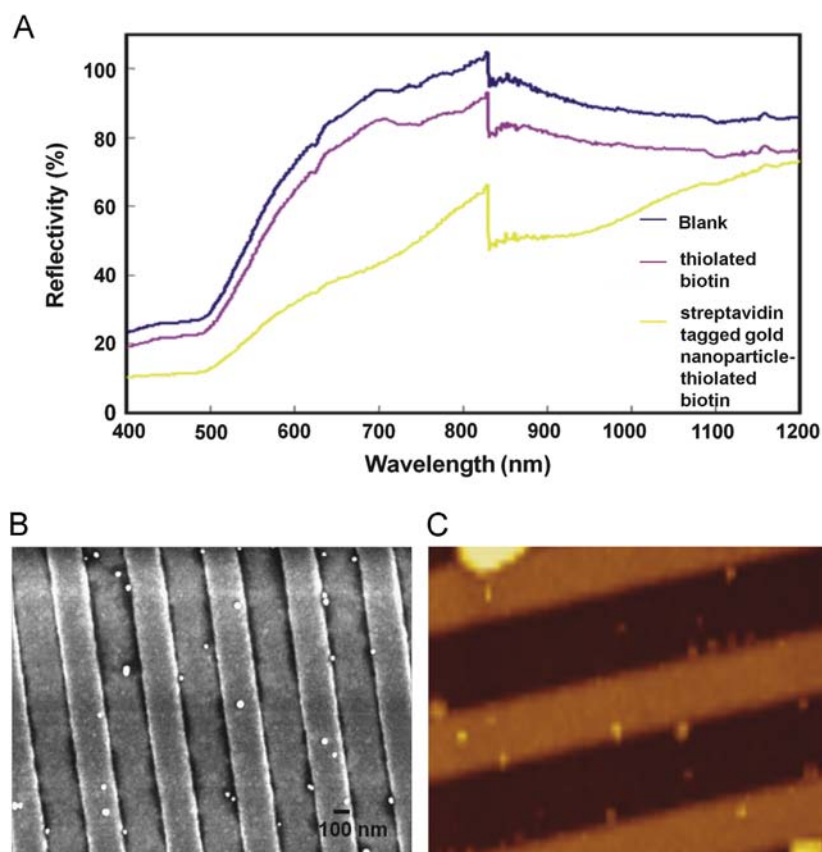


**Fig. 3.** (A) Reflectance measurement of streptavidin-tagged AuNPs and thiolated biotin on the surface of Au-coated polycarbonate. (B) SEM image analysis. (C) AFM image analysis. The images of tracks on the surface of the gold-coated polycarbonate account for the presence of tracks on the surface of polycarbonate used for data storage in DVD.

### 3.3. Biotin and streptavidin interaction on the surface of Au-coated polycarbonate

We monitored the binding reaction between streptavidin and biotin using UV–vis–NIR spectroscopy to ensure that our spectral method of measuring biomolecular interactions (immobilization and binding) is effective. In this study, biotin was linked to the thiol group and streptavidin was conjugated to AuNPs. Upon immobilization of thiolated biotin onto the surface of the Au-coated polycarbonate, reflectivity decreased by 10% (from 100% to 90%) (Fig. 3A). Interaction of this thiolated biotin with streptavidin-conjugated AuNPs caused the reflectivity to decline by 25% (from 90% to 65%). These data illustrate the decrease of reflectivity values associated with both immobilization and binding with biomolecules. Thus, spectral measurement can be used to monitor immobilization of biomolecules and their binding reactions. In addition, SEM and AFM image analyses were conducted to visualize the capturing of streptavidin-conjugated AuNPs by thiolated biotin on the surface of Au-coated polycarbonate. These images revealed that AuNP-tagged streptavidin was captured by thiolated biotin on the surface of the Au-coated polycarbonate (Fig. 3B and C). This capturing efficiency is attributable to the high dissociation constant of streptavidin and biotin, which is in the range of  $4 \times 10^{-14}$  M [19].

### 3.4. Interaction between anti-EPO and AuNP-tagged EPO on Au-layered polycarbonate

Western blot analysis showed that specific binding between monoclonal anti-EPO antibody and EPO occurred (Fig. 4A). After attachment of MHA-linked anti-EPO antibody to the Au-layered polycarbonate surface, capture of the EPO-tagged AuNPs by the

sensor was performed. UV–vis–NIR spectroscopy was used to monitor the interaction between the AuNP-tagged EPO and the anti-EPO antibody on the surface of the Au-coated polycarbonate (Fig. 4B). The interaction between the AuNP-tagged EPO and the anti-EPO antibody changed the reflectivity by 5% (95% to 90%). The change associated with this interaction was 5-fold less than that caused by the interaction between thiolated biotin and AuNP-conjugated streptavidin; this difference is likely due to the high affinity of the biotin–streptavidin interaction compared to that of EPO and anti-EPO antibody. Exploiting AuNPs in tagging EPO can increase the sensitivity of the detection due to the polyvalency of the EPO-tagged AuNPs, which have higher affinity than that of the EPO monomer itself because each AuNP is covered with more than one EPO molecules [20]. Thus, the use of AuNPs will definitely enhance the sensitivity of diagnostic devices [21]. However, in this study the main purpose of tagging EPO with AuNPs was to permit direct visualization of the EPO captured by the immobilized anti-EPO antibody by SEM and AFM.

### 3.5. SEM and AFM

SEM and AFM were used to obtain accurate images of the interaction between anti-EPO antibody immobilized on the surface of the platform and EPO-tagged AuNPs as well as morphologies of the surface of Au-coated polycarbonate. Fig. 4C shows an SEM image of the interaction between antibody and EPO. Because SEM only provides information about the lateral characteristics of the surface, AFM scanning was used to reveal the properties of the sample in the vertical direction. The AFM images showed that EPO-tagged AuNPs were captured by anti-EPO antibodies on the Au surface (Fig. 4D). These images also illustrate that tagging of the

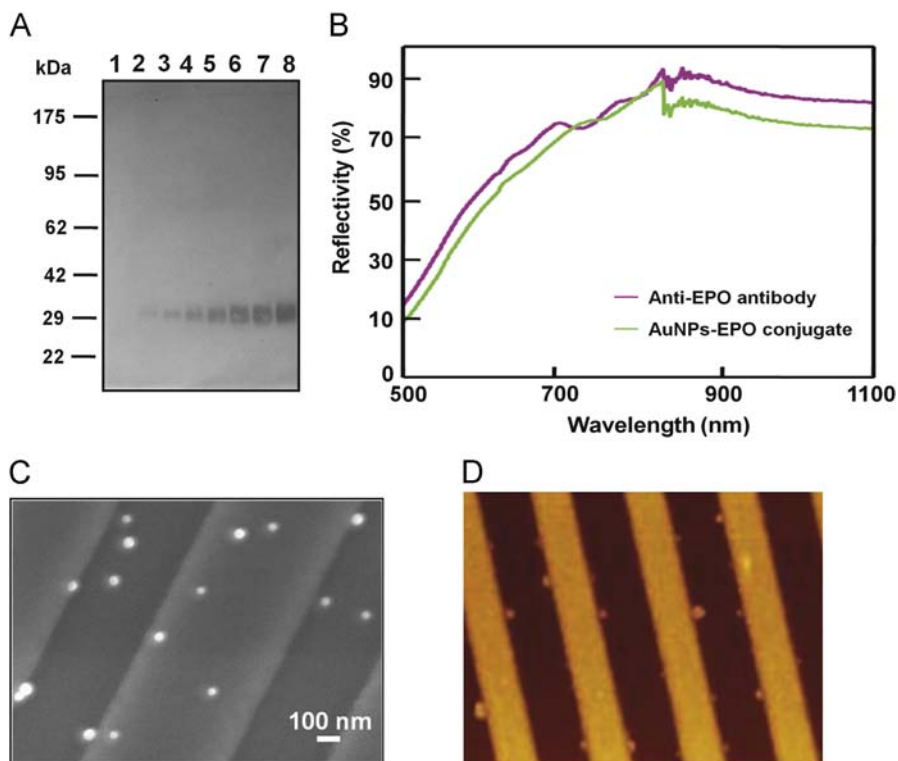


**Fig. 4.** (A) Western blot analysis of the EPO–anti EPO antibody interaction. Lane 1:  $9.76 \times 10^{-4}$ , Lane 2:  $1.95 \times 10^{-3}$ , Lane 3:  $3.91 \times 10^{-3}$ , Lane 4:  $7.81 \times 10^{-3}$ , Lane 5:  $1.56 \times 10^{-2}$ , Lane 6:  $3.12 \times 10^{-2}$ , Lane 7:  $6.25 \times 10^{-2}$ , Lane 8:  $1.25 \times 10^{-1} \mu\text{g}$ . (B) Reflectivity measurement of the interaction of anti-EPO antibody and EPO on Au-coated polycarbonate. (C) SEM image analysis. (D) AFM image of the AuNP-tagged EPO–anti EPO antibody interaction. The images of tracks on the surface of the gold-coated polycarbonate account for the presence of tracks on the surface of polycarbonate used for data storage in DVD.

antibodies with MHA-derived functional groups enables immobilization of biomolecules on the surface of Au-coated polycarbonate for subsequent capture of the target protein. (Inset Fig. 4).

### 3.6. Interaction between EPO and the anti-EPO DNA aptamer

Prior to taking UV–vis–NIR spectroscopy measurements, EPO–anti-EPO DNA aptamer complex formation was analyzed by performing the gel shift assay using native PAGE. The EPO–anti-EPO DNA aptamer complex has a higher molecular weight than EPO, causing the movement of the complex to be retarded and to move comparatively slower than EPO alone. Fig. 5A shows the specific formation of the DNA aptamer–EPO complex. Due to the limited detection level of ethidium bromide, at least 500 ng of DNA must be used with a higher concentration of target protein (up to  $\mu\text{M}$  level) to enable clear visualization of the formation of DNA–protein complex.

As the first step, the DNA aptamer extended with poly dA<sub>20</sub> dissolved in 1 × HEPES solution was denatured. Upon cooling to RT, this DNA aptamer formed secondary structures that can reside in the clefts or binding sites on the surface of EPO. As seen in Fig. 5B, the addition of poly dA<sub>24</sub> to 3′-end of the DNA aptamer did not change the stem loop structure originally retained by the DNA aptamer without poly dA<sub>24</sub>. Likewise, a similar binding reaction was executed on the surface of 30 nm Au-coated polycarbonate (Fig. 6A). Attachment of the thiolated poly dA<sub>20</sub> DNA aptamer resulted in reduction of the reflectivity by 5% (from 95% to 90%), whereas attachment of EPO caused the reflection to decrease by 10% (90% to 80%) (Fig. 6B). Thus, this set-up can be used to capture specific targets by the immobilized aptamer/antibody and to monitor the interaction using UV–vis–NIR spectrophotometry in a label-free manner. Moreover, a miniaturized version of the Au-coated polycarbonate (in the range of mm level, in the form of a

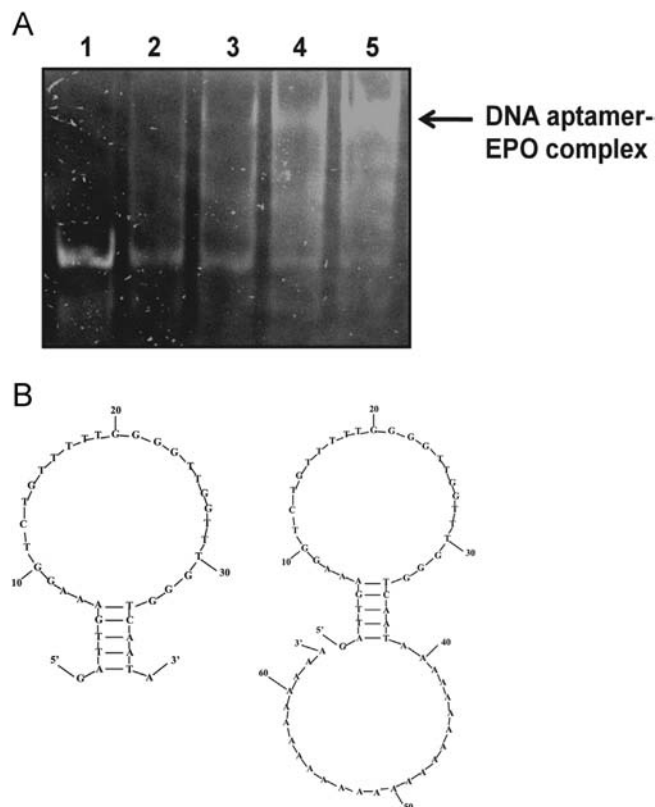


**Fig. 5.** (A) Gel shift assay of 4  $\mu\text{M}$  of anti-EPO DNA aptamer with increasing concentrations of EPO. Lanes 1–5: Concentrations of EPO protein were 0, 2, 4, 8, and 16  $\mu\text{M}$ . (B) Secondary structure of the anti-EPO DNA aptamer in the presence and absence of poly dA<sub>24</sub>.

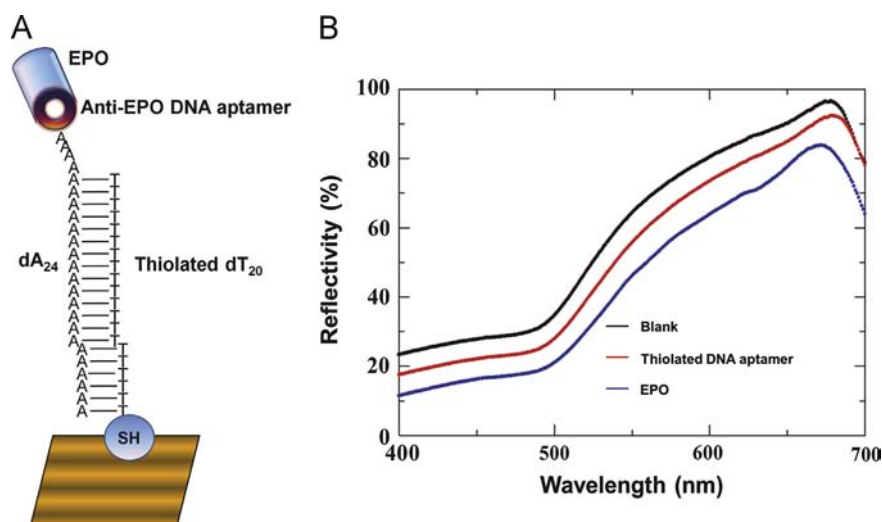


**Fig. 6.** (A) Cartoon illustration of thiolation of the anti-EPO DNA aptamer via nucleic acid duplex formation between anti-EPO DNA aptamer-poly dA<sub>24</sub> and thiol-poly dT<sub>20</sub> as well as binding of the EPO to the immobilized aptamer on the surface of Au-coated polycarbonate. (B) Reflectance measurement of the EPO and anti-EPO DNA aptamer interaction performed on Au-coated polycarbonate.

mini-chip) can be developed from this set-up. In this study, the Au-coated polycarbonate substrates used for analysis were cut into pieces so that the sizes suited the spectrophotometer's slit size. Another advantage of this system is that the protein captured by the immobilized aptamer can be recovered by eluting with elution buffer, and the immobilized aptamer can be reused for subsequent capture of the target protein.

#### 4. Conclusions

UV-vis-NIR spectroscopy was used successfully to track the interaction between EPO and its corresponding MREs (anti-EPO antibody and anti-EPO DNA aptamer) on the surface of Au-coated polycarbonate. We have shown that a 30 nm thick Au layer sputtered onto polycarbonate material to which the MREs are attached can be a useful element of a biosensor designed to capture EPO. Moreover, the Au-coated polycarbonate platform aided by UV-vis-NIR spectrophotometry can be used to monitor many other biomolecular interactions.

#### Acknowledgments

We thank Universiti Sains Malaysia (USM) for awarding an Academic Staff Training Scheme to Citartan to conduct this study. We are grateful to USM for providing support for his traveling and subsistence costs while in Japan. TH Tang was supported by USM Research University Grant 1001/CIPPT/813043. Y. Chen was supported by the following Grants: UM-MoHE HIR H-18001-00-C00020

and UM-MoHE HIR H-18001-00-C00009. Authors thank Research Committee, AMDI for the support of external English editing services.

#### References

- [1] J.P. Chambers, B.P. Arulanandam, L.L. Matta, A. Weis, J.J. Valdes, *Curr. Issues Mol. Biol.* 10 (2008) 1–12.
- [2] A.D. Ellington, J.W. Szostak, *Nature* 346 (1990) 818–822.
- [3] S.D. Jayasena, *Clin. Chem.* 45 (1999) 1628–1650.
- [4] C. Tuerk, L. Gold, *Science* 249 (1990) 505–510.
- [5] Z. Zhang, L. Guo, A. Guo, H. Xu, J. Tang, X. Guo, J. Xei, *Bioorg. Med. Chem.* 18 (2010) 8016–8025.
- [6] S.C. Gopinath, R. Kumaresan, K. Awazu, M. Fujimaki, M. Mizuhata, J. Tominaga, P.K. Kumar, *Anal. Bioanal. Chem.* 398 (2010) 751–758.
- [7] J.W. Fisher, *Exp. Biol. Med.* 228 (2003) 1–14.
- [8] R. Rivier, M.J. Saugy, *J. Toxicol. Toxin Rev.* 18 (1999) 145–176.
- [9] A. Biswas, Z. Marton, J. Kruse, J. Kanzow, V. Zaporozhtchenko, F. Faupel, T. Strunskus, *Nano Lett.* 3 (2003) 69–73.
- [10] N. Kumari, S.B. Krupanidhi, K.B.R. Varma, *J. Mater. Sci. Mater. Electron.* 21 (2010) 1107–1114.
- [11] S.V. Rao, K.W. Anderson, L.G. Bachas, *Microchim. Acta* 128 (1998) 127–143.
- [12] T.T. Le, C.P. Wilde, N. Grossman, A.E. Cass, *Phys. Chem. Chem. Phys.* 5271 (2011) 5271–5278.
- [13] T.M. Willey, A.L. Vance, T. van Buuren, C. Bostedt, A.J. Nelson, L.J. Terminello, C. S. Fadley, *Langmuir* 20 (2004) 2746–2752.
- [14] M. Frascioni, F. Mazzei, T. Ferri, *Anal. Bioanal. Chem.* 398 (2010) 1545–1564.
- [15] J.V. Staros, R.W. Wright, D.M. Swingle, *Anal. Biochem.* 156 (1986) 220–222.
- [16] S. Xu, S.J.N. Cruchon-Dupeyrat, J.C. Garno, G.Y. Liu, G.K. Jennings, T.H. Yong, P. E. Laibinis, *J. Chem. Phys.* 108 (1998) 5002–5012.
- [17] M. Mrksich, *MRS Bull.* 30 (2005) 180–184.
- [18] L.H. Chen, Q. Wang, W.G. Hou, *Afr. J. Biotechnol.* 24 (2009) 7148–7155.
- [19] N.M. Green, *Methods Enzymol.* 184 (1990) 51–67.
- [20] W.P. Hall, S.N. Ngatia, R.P. Van Duyn, *J. Phys. Chem. C* 115 (2011) 1410–1414.
- [21] F. Rusmini, Z. Zhong, J. Feijen, *Biomacromolecules* 8 (2007) 1775–1789.